AD-A185 526 STUDIES OF THE STRUCTURAL DYNAMIC BEHAVIOR OF SATELLITE 1/1
ANTENNA SYSTEM(U) RENSSELAER POLYTECHNIC INST TROY NY
R G LOEWY 29 JUN 87 AFOSR-TR-87-1167 $AFOSR-83-0348

UNCLASSIFIED F/G 22/2 NL

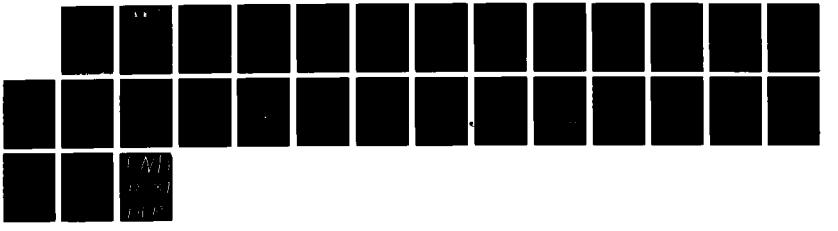

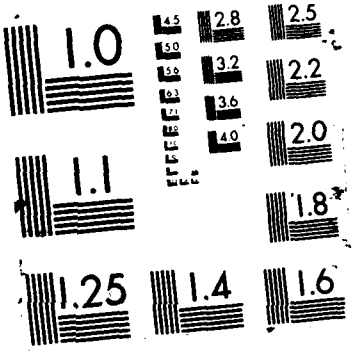
1.0
1.1
1.25
1.4
1.6
1.8
2.0
2.2
2.5
2.8
3.2
3.6
4.0
4.5
5.0
5.6
6.3

SECURITY CLASSIFICATION OF THIS PAGE

AD-A185 526

REPORT DOCUMENTATION PAGE

DTIC ELECTE OCT 0 1 1987 S D

1b. RESTRICTIVE MARKINGS	
2a. SECURITY CLASSIFICATION AUTHORITY	3 DISTRIBUTION / AVAILABILITY OF REPORT Approved for Public Release; Distribution Unlimited.
2b. DECLASSIFICATION / DOWNGRADING SCHEDULE	
4. PERFORMING ORGANIZATION REPORT NUMBER(S)	5. MONITORING ORGANIZATION REPORT NUMBER(S) AFOSR-TR- 87-1167
6a. NAME OF PERFORMING ORGANIZATION Rensselaer Polytechnic Inst.	6b. OFFICE SYMBOL (If applicable)
6c. ADDRESS (City, State, and ZIP Code) Troy, N.Y., 12180	7a. NAME OF MONITORING ORGANIZATION Air Force Office of Scientific Research
	7b ADDRESS (City, State, and ZIP Code) Bldg. 410 Bolling AFB, DC 20332-6448
8a. NAME OF FUNDING / SPONSORING ORGANIZATION AF Office of Scientific Research	8b. OFFICE SYMBOL (If applicable) NA
	9. PROCUREMENT INSTRUMENT IDENTIFICATION NUMBER AFOSR 83-0348
8c. ADDRESS (City, State, and ZIP Code) Bldg 410 Bolling AFB, DC 20332-6448	10. SOURCE OF FUNDING NUMBERS

PROGRAM ELEMENT NO.	PROJECT NO.	TASK NO.	WORK UNIT ACCESSION NO.
61102F	2302	B1	

11. TITLE (Include Security Classification)
Studies of the Structural Dynamic Behavior of Satellite Antenna Systems (Unclassified)

12. PERSONAL AUTHOR(S)
Robert G. Loewy

13a. TYPE OF REPORT	13b. TIME COVERED	14. DATE OF REPORT (Year, Month, Day)	15. PAGE COUNT
Final	FROM 9/1/83 TO 6/29/87	1987, June 29	27

16. SUPPLEMENTARY NOTATION

17 COSATI CODES			18. SUBJECT TERMS (Continue on reverse if necessary and identify by block number)
FIELD	GROUP	SUB-GROUP	Satellite Antenna, Hoop-Column or Hoop Maypole Antenna, Structural Dynamics, Free Vibrations, Transfer Matrix Analysis

19. ABSTRACT (Continue on reverse if necessary and identify by block number)

A Transfer Matrix (TM) Analysis is formulated to predict the natural modes and frequencies of hoop-maypole type satellite antenna systems. Two directions of bending, axial extension/compression and torsion are represented as coupled by feed assemblies canted with respect to the mast, solar panels tilted out of the plane of the center structure and masses offset from the mast centerline. Shear deflections, large steady cable loads and large compressive loads are accounted for in appropriate members. Using properties chosen as representative of such structures, trends are predicted with variations in size and configuration for several simplified configurations; these include, (a) two-dimensional cable-suspended rigid bars on a flexible center body (mast), (b) "T" and "H"-shaped center body substructures in two- and three-dimensional vibrations and (c) cable-stiffened, planar polygonal hoop assemblies. In the last of these "cyclic symmetry" had to be invoked to avoid numerical difficulties. Some general conclusions are drawn regarding the free vibrations of such structures. The TM approach is seen as a viable alternative to FEM analyses, when structures are encountered which have major substructures with one dimension longer than its others. Full use of the TM analysis for hoop-maypole type structures must await a reformulation in which "cyclic symmetry" can be invoked, as in the plane hoop cases.

20. DISTRIBUTION / AVAILABILITY OF ABSTRACT	21. ABSTRACT SECURITY CLASSIFICATION
☒ UNCLASSIFIED/UNLIMITED ☐ SAME AS RPT ☐ DTIC USERS	UNCLASSIFIED

22a. NAME OF RESPONSIBLE INDIVIDUAL	22b TELEPHONE (Include Area Code)	22c. OFFICE SYMBOL
ANTHONY K. AMOS	(202) 767-4937	AFOSR/NA

DD FORM 1473, 84 MAR 83 APR edition may be used until exhausted. All other editions are obsolete.

SECURITY CLASSIFICATION OF THIS PAGE

87 9 24 083

AFOSR-TR- 87-1167

Final Report
Grant No. AFOSR-83-348

Studies of the Structural Dynamic Behavior of Satellite Antenna Systems

I Introduction

The "hoop-column" or "hoop-maypole" type of antenna (Fig. 1.) is typical of many of the space structures being designed and anticipated for use in near-earth orbit. The natural modes and frequencies of such sparse structures, which are exceptionally large and light (i.e., flimsy by earthly standards), must be known with considerable accuracy to insure that corrective impulses (or other control forces and moments), as applied by vernier thrusters or control gyros, will not inadvertently trigger unstable closed-loop oscillations.

Motivation for the subject studies were two fold: first, to gain some insight as to the changes in natural modes and frequencies with large variations in design parameters; and second, to develop a transfer matrix method of analysis as an alternative to finite element methods (FEM) which are presently the primary analysis tool in dealing with the dynamic response of complex space structures. Straightforward applications of powerful analysis approaches such as the finite element method leave much to be desired. The results are usually of such volume and complexity as to obscure the nature of the responses and hinder the proper choice of design changes. A structural breakdown sufficient for accuracy in such analyses is also costly in manhours and computer time. The transfer matrix approach promises efficiency at a level which is appropriate for a practical design tool; at the same time its modular nature may increase insights and understanding regarding the dynamic behavior of flexible space structures.

The work reported here was conducted in several phases; (a) formulation of the complete analysis, (b) two-dimensional trend studies of flexible beam-columns from which a rigid bar is suspended by cables, (c) two and three-dimensional trend studies of "T" and "H" structures typical of various combinations of substructure consisting of mast, feed assemblies and solar panels, (d) trend studies of the modes and frequencies of planar, polygonal, cable-stiffened "hoop" structures and (e) investigations into the numerical difficulties enountered. Fig. 2 (from Ref. 1) is representative of the kinds of variation likely to be encountered in design studies.

II Results

Phase A (Theoretical Development)

The first phase resulted in a transfer matrix formulation in which bending in two normal directions, compression/extension, and torsion are all represented in the major structural components of the system; namely feed assembly, central column (or mast), hoop and solar panels. Cables are assumed to run from the vertices formed by the ends of each hoop element to three different longitudinal stations on the central mast; they are treated as massless springs in which there are (large) preloads. The portion of the mast between hoop-cable attachments carries a (large) steady, compression load, as do the hoop's polygonal sides. The feed assemblies are treated as attached to the mast at an angle of 90°, but also have an arbitrarily large "bend" built into them, to account for "aiming" their E-M radiation properly at the reflecting surface. The solar arrays are treated similarly, but here an arbitratily large,

discreet "twist" is introduced to account for their being oriented toward the sun. Shear deflections are accounted for, as well as mass-offsets, which have the consequence of eliminating symmetry.

The full analysis, then, involves 12 x 12 transfer matrices, which successively premultiplied, as unknown state vectors are eliminated, lead to a 6 x 6 determinant whose value should be zero for the correct choice of a trial frequency. The solution procedure, therefore, is to - by trial and error - find the frequencies which make this determinant zero (Ref. 2).

All the results reported below for the phases of the project subsequent to this one used special, more limited cases of the theory developed in Phase A.

Phase B (Two Dimensional Dynamics of a Rigid Bar Cabled to a Flexible Mast)

For this phase of the research, more fully reported in Ref. 3, the baseline antenna configuration was assumed to have the characteristics given in Table 1, and no steady load in the cables. The mathematical model for the flexible mast had five discreet masses outside the cable attachment points and 9 inside them for a total of 19 masses. In all mast length variations, the mass per unit length was held constant; in hoop (rigid bar) length variations, the mass per unit length was held constant but its mass moment of inertia was assumed to vary as that of a rigid circular hoop. Changes in natural frequencies as the mast length varies are shown in Figs. 3a and b. These configurations are symmetric above and below and hold the portion of mast length between cable attachments constant. The odd numbered bending modes are symmetric modes; those even numbered are antisymmetric about the configuration's center. The half-structure analysis, using appropriate boundary conditions for symmetry and antisymmetry gave results identical (as expected) to those of the full structure and resulted in 30% computer running time savings. Proper boundary conditions for the half structure are;

For the symmetric case:
- at the mast center -
  - lateral bending slope = 0
  - lateral shear force = 0
  - axial displacement = 0
- for the half bar -
  - rotation = 0
  - x and y components of cable force equal the D'Alembert forces due to those components of the (one half) bar's translation

For the antisymmetric case:
- at the mast center -
  - lateral displacement = 0
  - bending moment = 0
  - axial force = 0
- for the half bar -
  - bar center displacement = 0
  - the cable force components perpendicular to the bar times the bar length equal the D'Alembert moment due to the (one half) bar rotation.

When the length of the mast above the cable attachment points is varied (ie the length of the "feed mast"), keeping its mass/length and all other mast properties constant, one obtains the trends shown in Figs. 4a and 5. This is one of three kinds of asymmetry (lengthwise) examined in Ref. 3. Among other trends similarly calculated were the effect of varying bending stiffness outside the cable attachment points relative to that inside, the rigid hoop (bar) length and cable attachment angles. Trends where the large steady axial load in the mast between cable attachments was added and varied relative to its Euler buckling load were also obtained. While frequencies dropped, as expected, no significant mode shape changes occurred to within a factor of 2 of the buckling load. To assess the effects of moving a suspended hoop (bar) from its centrally attached position, all the mast properties were held constant, and the cable attachment points moved axially to various offsets from the initially symmetric position. Cable angles, bar(hoop) length, etc all remained unchanged. The resulting variations are shown in Fig. 5a and b. (In these figures P_a = axial compressive load in the length of Central Column between cable attachments, and P_B = the critical buckling load in that member.) The existence of steady axial loads induced by cable tension is more influential as symmetry is lost for some modes, and less influential in others. A total of 32 different configurations are considered in Ref. 3 with up to 10 natural modes and frequencies given for each configuration.

This simple model provides a useful reminder that for such systems, the classical count of nodes (points of zero deflection) is only a reliable indicator of modal number if one can make a separation between modes primarily involving the continuous structure and those involving soft-sprung substructures. This is clearly shown in Figs. 6a, b and c.

Phase C (Two and Three Dimensional Dynamics of "T" and "H" Substructures)

This phase continued studies of component substructure dynamic behavior; first, the "T" formed by the feed assemblies or the solar panels mounted on a central mast, and then the "H" (really on its side) formed by the feed assemblies, mast and solar arrays. These were first examined as two-dimensional structures. Tables 2, 3 and 4 list the properties used, which were arrived at on the basis of some known dimensions and materials and assumptions intended to be compatable with those of the hoop maypole antenna described in Ref. 4. Both "T" and "H" substructures can be symmetric, and for such cases the half-"T" and half-"H" were analyzed and identical results obtained with check calculations using the full structure (to within four places of ω_n value). Proper boundary conditions for the "T" and the "H" where the full symmetric structure is split, ie along the center of the mast, are:

for the symmetric case -

Transverse Shear Force	= 0
Bending Moment	= 0
Bending Slope	= 0
Lateral Displacement	= 0

for the antisymmetric case -

Axial Displacement	= 0
Axial Force	= 0

Boundary conditions were zero force and moment at the free ends of both structures; the base of the "T", however, was assumed to be cantilevered, ie zero deflections and rotations at that point.

Changes in frequency and mode shapes were calculated as the lengths of feed assemblies and solar panels were varied, and for these cases of the "T" substructures, some general characteristics can be cited.

- o Solar panels are so flexible in transverse bending motion, that no axial extensions of the mast are perceptable in symmetric transverse bending motions up to the sixth mode.

- o The Solar Panel "Base's" transverse bending rigidity (or lack of it) is such that the "continuity of slopes" required of symmetric mode shapes appears to be violated (and is not).

- o Solar Panel Mass/Stiffness distributions are such as to result in unusually low vibratory deflections near the free ends in the first six modes.

- o The order of feed assembly/upper mast modes (1^{st} & 2^{nd} antisymmetric, 3^{rd} symmetric, 4^{th} & 5^{th} antisymmetric, 6^{th} symmetric) is unchanged as feed assembly length is varied from 1/2 to 3 times the base case (with constant mass/unit length).

- o The 6^{th} feed assembly/upper mast mode (2^{nd} symmetric) shows significant axial mast motion; the smaller the feed assembly, the greater this motion.

- o Reduction in CPU time using the half "T" compared to the full "T" was 26.5%.

Variations of the symmetric "H" substructure included solar panel length increases (outward) to 130% of its base case; increasing solar panel length inward ie shortening attachment and foundation arms commensurately) to 130%; increasing mast length to 163%, increasing mast stiffness by factors up to 8, increasing feed assembly stiffness by factors up to 6 and length (hence mass) changes of from 1/2 to 3 times the base case. Several general conclusions can be drawn as regards the first six natural modes and frequencies.

- o they appear to be dominated by mast and feed assembly mass and by solar panel (plus attachment) flexibility.

- o the order of modes, first antisymmetric, then alternating to the sixth (which is symmetric) is unchanged throughout the complete range of parameter variations.

- o consistent with the alternating (antisymmetric/symmetric) nature of the first six modes and the mass dominance of the mast and feed assembly, natural frequencies are closely "paired". That is, each pair of symmetric and antisymmetric modes are close in frequency, with the usual sort of frequency separation (factors of 2 to 3) between one pair and another.

- o the effect of the mast stiffness changes were not reflected in natural frequencies (to four places) and were imperceptable in the mode shapes.

- o the effect of feed assembly stiffness and length (and therefore mass) changes were perceptable, but very slight.

Additional trends were obtained for changes which destroyed the symmetry of the "T" and "H" substructures. For the "T" cases examined, such changes caused the two sides (feed assemblies or solar arrays) to behave much more independently. For the "H" cases, the symmetry/antisymmetry mode-type alternation was broken and so was the frequency "pairing".

Complete results are given in Ref. 5, where a total of 31 configurations are considered and up to six natural mode shapes and frequencies are given for each. This includes ten configurations of the "T" substructure and twenty-five configurations of the "H" substructure, of which ten are asymmetric.

To examine the fully-coupled, three dimensional free vibration behavior of the feed assembly, mast, and solar assembly ("H" substructure), the 100-meter hoop-column antenna of Ref. 4 was considered. The properties used to model the "H" substructure of the 100 meter antenna are shown in Table 5. The subscripts "v" and "w", here, signify in-plane and out-of-plane (relative to the plane of the antenna) properties, respectively. In the case of the solar panels, in-plane and out-of-plane designations refer to the planes of the panels themselves. Values of certain geometrical and material properties for the 100-meter antenna model were arrived at by scaling properties of the 15 meter model described in Ref. 6. As a consequence of the lack of information on specific solar panel configurations being considered in the design of the 100-meter hoop-column antenna, a solar assembly design discussed extensively in the literature[7,8,9], was chosen for the analysis. This design, referred to as the solar electric propulsion (SEP) array is capable of generating 25 kW of power. The SEP, as modelled here, consists of three main subcomponents as shown in Fig. 1. These are the two solar arrays themselves, which each consist of triangular extendable lattice structure masts which support flat-fold flexible panels, the solar boom, which is the canister that the extendable mast is stored within prior to deployment, and the base, which contains such equipment as the solar array rotational drive. A description of the scaling process used, as well as additional explanations for the choice of antenna properties together with all the analysis results are presented in Ref. 10. The properties displayed in Table 5 represent the "base" set from which parametric variations were performed.

For three-dimensional analysis of a symmetric "H" substructure, only one half of the mathematical model need be analyzed, much as in the two-dimensional case. The pertinent three-dimensional, half-"H" mathematical model is shown in Fig. 7. The appropriate boundary conditions on the center body are

for the symmetric case:

$$\text{all inplane bending state variables} = 0$$
$$\text{all torsion state variables} = 0$$

for the antisymmetric case:

$$\text{all out-of-plane bending state variables} = 0$$
$$\text{all extension compression state variables} = 0$$

The effect of changes in bending stiffness of the feed assembly, equal in in-plane and out-of-plane directions on natural frequencies were calculated and are plotted Fig. 8. This shows (and mode shapes confirm) that the feed assembly stiffness value of about 10^5 N-m^2 divides a region below which the first symmetric mode involves primarily feed assembly motion and above which it involves primarily solar panel motion.

The effect of solar panel angle and boom stiffness variations on antisymmetric mode frequencies was predicted and is shown in Fig. 9. It is clear that boom stiffness plays a significant role in these trends; at values of 5.10^5 N-m^2 and below, the mode shapes show the solar panels to behave as rigid bodies in the first three antisymmetric modes, so that their orientation doesn't affect the corresponding natural frequencies, primarily involving, as they do, the flexibility of the circular cross sectioned solar booms. At boom stiffness values of $3x10^7$ N-m^2 and above, flexible motions of the solar panels and the mast begin to be important, and their relative orientations thus vary these fundamental frequencies.

Variations in the lowest four natural frequencies were examined as a result of the coupling introduced by a mass suspended from the feed-mast junction but offset laterally (out-of-plane) from the mast center line at varying distances. This makes the entire three-dimensional "H" substructure asymmetric. The value of this mass was taken as 8% of the mast mass. Results are shown in Fig. 10. Namely, only the fourth mode frequency was affected. This overall lack of impact for substantial offsets was unexpected. When it was influential, ie in the fourth mode, the mode shape indicated this was through increased axial tension/compression in the mast coupling with out-of-plane bending.

In all, /Ref. 10 provides up to four fully-coupled, three-dimensional, free vibration mode shapes and frequencies for each of twenty-one different "H" substructure configurations.

Phase D (In and Out-of-Plane Dynamics of Cable-Stiffened Polygonal Hoops)

This phase of the research investigated application of the transfer matrix method to the determination of the free vibration behavior of a series of cable-stiffened hoop platforms. Hexagonal spacecraft subassemblies of this kind were studied by Belvin[11] both experimentally and using a NASTRAN analysis.

In this analysis (as in the complete development of Phase A), cable stiffeners were "divided into half" and applied at both ends of a hoop segment, so that the transfer represented by the matrix [T] would be symmetric, so far as cable stiffeners were concerned. Note that the cable intersection point is considered fixed to "ground" in these studies; in Ref. 11, that point is free.

Transferring completely "around" this substructure i.e., successively across all of the hoop segments, leads to the requirement for the structure to "close" on itself. Compatability of displacements and equivalence of forces and moments, lead to a matrix form of the characteristic equation of the system. For example, by first calculating the matrix [T] - representing the transfer from the state vector at one end of a hoop segment (station j) to that at the other (station j+1) - raised to the N^{th} power, where N is the number of hoop segments, the following relation may be written:

$$[z]_{j+N} = [T]^N [z]_j$$

However, since $[z]_{j+N}$ must equal $[z]_j$, this equation may be rewritten as

$$([I]-[T]^N)[z]_j = 0$$

For $[z]_j$ to be non-zero, the determinant of $([I]-[T]^N)$ must vanish for trial frequencies corresponding to the natural frequencies of the hoop.

Rather than a straightforward manipulation of the determinant of $\{[I]-[T]^N\}$, however, we found it possible to determine the natural frequencies and mode shapes of the whole hoop substructure by considering the relationship between the modal behavior of the smallest repeating element (i.e., one hoop segment including half-cables at either end) and the remaining elements, using Thomas' method of cyclic symmetry[12]. This is done by defining a complex hoop joint state vector and linearly combining two sets of state variables corresponding to modes which are orthogonal and which have the same natural frequency. That is:

$$[z]_j = [s]_j + i[\bar{s}]_j \quad \text{where} \quad i = \sqrt{-1}$$

The periodicity of closed cyclically symmetric bodies makes it possible to relate the state vectors at the ends of hoop elements as follows:

$$[z]_j = e^{i\gamma}[z]_{j-1}$$

where γ must assume one of the values:

$$\gamma = 2\pi n/N$$

where n is an integer. The phase angle, γ, may have (N/2+1) possible independent values for N even and (N+1)/2 values if N is odd.

Since, the transfer relations require that $[z]_j = [T][z]_{j-1}$ the cyclic symmetry relation allows writing

$$((\cos\gamma + i\sin\gamma)[I] - [T])[z]_j = 0$$

or: $[D][z]_j = 0$

and for this relation to have a non-trivial solution, $[z]_j \neq 0$, the determinant of [D] must vanish. The values of ω which make [D] = 0 correspond to the natural frequencies of the full hoop.

In-plane and out-of-plane natural frequencies were obtained using this analysis for hoops with 5 through 11 sides. Tables 6 and 7 show the properties of the hoop analyzed and compare the present results and those of Belvin[11], respectively. Figures 11a and b show the effect of altering the number of segment sides on the first six in-plane and out-of-plane natural frequencies of the 1 meter radius hoop. The in-plane frame stiffening brought about by raising the number of segments (and thus cables) of the constant diameter hoop is demonstrated; fairly steady rise in the first six in-plane frequencies can be observed as the number of hoop segments is increased. Since this analysis assumes first order small displacemnets, out-of-plane vibrations are influenced less consistantly by cable stiffness.

Both mode shapes and frequencies were calculated for 5,6,8, and 11 sided hoops and are presented with full discussion of the results in Ref. 13. Note that torque and moment balance about the cable intersection point was not always obvious in these modes, (see, for example, the first in-plane and out-of-plane modes for the pentagonal hoop in Figs. 12a and b) but computations confirmed such equilibrium in all cases.

Comparison of computer "problem state CPU times" for the subject method as compared to Belvin's NASTRAN program[11], are estimated to be, for ten modes and frequencies, 6.1 secs and 42.3 secs, respectively, for one configuration.

Phase E (Investigations of Numerical Difficulties)

The full hoop-maypole antenna model described in Fig. 1 and Phase A of this report was programmed for solution on an IBM 3081-D. Static solutions were run to confirm the internal equilibrium of cable tension loads and hoop and mast compression loads. These satisfactory checks lent confidence as to programming accuracy.

Attempts to run natural frequencies, however, ran into numerical difficulties. These were evidenced by lack of any reasonable continuity in the curves of determinental values versus trial frequencies; rather such plots appeared to be a scattering of random points. Initial checks of the validity of inverses within the program showed that the difficulties were not there. Since the determinental values are customarily calculated as small differences between large numbers, double precision had been used at the outset. The authors of Ref. 2 offered a modification to the trial and error procedure for finding natural modes and frequencies, which ameliorates the "small differences between large numbers" problems. Essentially it consists of assuming a state vector at one of the boundaries (the "near" end) with each assumed value of trial frequency ω, and carrying a correction column with an unknown coefficient for the state vector. Iterations then are made on the state vector using values of the correction factor averaged from those (initially) different values, which result from conditions set by the known boundary conditions at the "far" end. (See Ref. 2 pages 204 through 213.) This modified scheme made no improvement in the numerical difficulties encountered.

In the studies of the isolated hoop structures reported, above, for Phase D, the most likely source of the numerical difficulties was revealed. The full antenna analysis of Phase A used the straightforward requirements of hoop "closure" discussed at the beginning of the Phase D report, above. The isolated hoop analysis began that way, as well.

This straightforward approach requires formation of the matrix $[T]^N$, as noted earlier. Uhrig[14] and Davies[15] have pointed out, however, that calculating the product of transfer matrices in a long chain of identical components (in this case the hoop segments with half-cables at each end) may lead to large errors, since all the columns of the matrix product $[T]^N$ tend to parallelism with the eigenvector associated with the dominant eigenvalue of the component matrix [T] as N becomes large. Note that this is inherent in the iteration technique for calculating characteristic values.

A method suggested by Davies to avoid the parallelism phenomena, involves the creation of a "supermatrix" which contains blocks of [T] along its diagonal. This large matrix is then used to obtain $[T]^N$ by Gaussian elimination. While this approach may be essentially free of numerical difficulties for non-closed periodic structures, problems still arose, in the form of erratic behavior of the determinant values, when this "supermatrix" scheme was applied to the hoop model. This suggests that there are some further inherent numerical difficulties present in the application of the transfer matrix method to closed cyclically symmetric structures. In this research it was only possible to avoid them by taking advantage of the symmetry of the structures, as demonstrated by the isolated hoop analysis in Phase D.

Thus, the transfer matrix analysis method developed in Phase A for complete hoop-maypole antenna structures would seem to require reformulation so as to allow the cyclic symmetry of the suspended hoop to be accounted for in the integrated structure, as it was for the isolated hoop.

In any event, the user of a transfer matrix analysis should be aware of the existence of asymptotes in the determinantal value vs trial frequency plots for mathematical models involving "branches", which provide multiple paths of transfer leading to the same point. A simple example of this kind is the "T" substructure discussed under Phase C, above. There are two paths by which the transfer procedure can reach the single juncture at the top of the "T". Thus, the determinantal value will change sign between the values of trial frequency that are on either side of the natural frequencies of the cantilever modes of one half of the top of the "T". This change of sign does not signify a natural frequency of the complete "T" substructure, however, as shown in Figure 13. While, at first glance, a complication in seeking modes for the complete system, knowledge of the position of these asymptotes, by partial analyses of any system, can provide guidance which could reduce total running time for the modes of a complete, multibranched system.

Conclusion

The research reported here has provided insight regarding the complexity of the natural modes and frequencies of hoop-maypole antenna systems by dealing, in some detail, with the free vibratory characteristics of some of its substructures and simplified versions of the integrated system. Some typical designs reveal solar panel support booms as being a critical structural element for some fundamental modes, and in others the mass of feed assemblies is shown to be a dominant factor. Cable stiffening effects are such that in-plane hoop modes are generally raised as the number of hoop elements is increased. For the kind of symmetry found in a typical design, symmetric and antisymmetric modes can be expected to be "paired", ie one of each kind found at nearly the same natural frequencies.

The transfer matrix analysis has been found to be a viable alternative to FEM analyses for the various substructures of the hoop-maypole type of satellite antenna. In fact, considerable computer running time and storage requirement reductions relative to NASTRAN can be expected. On the other hand, a complete analysis still awaits a reformulation of the integrated structure which takes advantage of the cyclic symmetry in the hoop platform, in order to overcome the numerical difficulties associated with analyzing closed, repetitive structures with the transfer matrix method.

Table 1

Two Dimensional Model Geometric Properties
For Baseline, Rigid Suspended Hoop, Symmetric Model

	Feed Mast(1)	Center Mast(2)	Solar Mast(3)
Length (in)	900	2500	900
Mass (lb)	540	1500	540
EI ($lb\text{-}in^2$)	16.24×10^9	16.24×10^9	16.24×10^9
EA (lb)	60.15×10^6	60.15×10^6	60.15×10^6

Solar Array and Feed Assembly Mass Taken as Zero.

Cable Spring Rates = 75#/inch

Rigid Hoop (Spring Suspended Bar): Mass = 800 lb

: Mass Moment of Inertia = 4×10^9 lb -in^2

(1) above cable attachments
(2) between cable attachments
(3) below cable attachments

Table 2

Base Case for the Upper "T" Substructure (See Fig. 1)

Section	Outboard Feed Arm	Intermediate Feed Arm	Inboard Feed Arm	Upper* Mast
Mass, kg	68.0	68.0	68.0	175.0
Length, m	1.7	1.7	1.7	25.0
EI, $N^2_m x10^{-6}$	1.81	1.81	1.81	25.40
EA, $Nx10^{-7}$	217.00	217.00	217.00	86.00

Table 3

Base Case for the Lower "T" Substructure (See Fig. 1)

Section	Solar Panel	Solar Panel Boom	Solar Panel Base	Lower Mast**
Mass, kg	20.0	5.6	305.6	60.0
Length, m	15.5	10.9	10.9	12.0
EI, $N^2_m x10^{-6}$	.001	.001	.001	13.30
EA, $Nx10^{-7}$	.001	3.44	3.44	68.80

Table 4

Base Case for the "H" Substructure

Section	Solar Panel	Solar Panel Boom	Solar Panel Base	Full Mast	Feed Assembly
Mass, kg	20.0	5.6	305.6	644.0	204.0
Length, m	15.5	10.9	10.9	92.0	5.1
EI, $N^2_m x10^{-6}$	.001	.001	.001	25.40	1.81
EA, $Nx10^{-7}$	.001	3.44	3.44	86.00	217.00

* from the upper cable attachment to feed assembly
** from the lower cable attachment to solar panels

Table 5

Properties of 100 Meter Antenna Components

Section	MASS (Kg)	LENGTH (m)	EA (N)	EIv ($N\text{-}m^2$)	EIw ($N\text{-}m^2$)	GJ ($N\text{-}m^2$)
Feed Assembly	792.5	3.8	$.1 \times 10^{11}$	$.1 \times 10^{11}$	$.1 \times 10^{11}$	$.1 \times 10^{11}$
Column	644.0	81.9	1.332×10^{7}	7.095×10^{9}	7.095×10^{9}	3.751×10^{9}
Base	242.0	1.1	$1. \times 10^{11}$	$1. \times 10^{11}$	$1. \times 10^{11}$	$1. \times 10^{11}$
Solar Boom	.0889	1.1	2.062×10^{9}	3.757×10^{7}	3.757×10^{7}	3.01×10^{7}
Solar	300.5	39.6	1.090×10^{9}	1.030×10^{10}	5.438×10^{7}	3.036×10^{9}

	I_v ($K_g\text{-}m^2$)	I_w ($K_g\text{-}m^2$)	J ($K_g\text{-}m^2$)
Solar Panel Mass Moments of Inertiz	160.15	34.28	117.7

Note: Stiffness values of $1. \times 10^{11}$ are intended to be effectively infinite.

Table 6 - Hoop segment and cable properties

Hoop Segments	
Mass/length:	.8755 kg/meter
Segment cross-sectional A:	3.2258×10^{-4} meter^2
EI in-plane:	76.96 Newton-meter^2
EI out-of-plane:	4925. Newton-meter^2
EA:	22.90 MNewton
GJ:	113.3 Newton-meter^2
Cables	
Cable Length:	1 meter
Stiffness:	1.693×10^5 Newtons
a Preload (in-plane case):	7.5954 Newtons*
b Preload (out-of-plane):	97.224 Newtons*

* Values shown correspond only to the hexagonal case:

[a] In-plane cable preload varies such that ratio of resulting compressive force in each hoop segment to its Euler buckling load remains at .01 as number of hoop sides is varied.

[b] Out-of-plane cable preload varies such that ratio of resulting compressive force in each hoop segment to its Euler buckling load remains at .002 as number of hoop sides is varied.

Table 7 - Comparison between NASTRAN and transfer matrix calculation results for the natural frequencies of the hexagonal hoop

In-plane

Mode	TM method	NASTRAN (Ref. 11)
1	92.1	92.1
2	116.5	116.6
3	162.0	a
4	210.0	210.1

Out-of-plane

Mode	TM method	NASTRAN (Ref.11)
1	59.00	58.41
2	129.00	128.10
3	740.00	740.30
4	955.00	947.60
5	1369.00	1355.00

[a] Not reported in Belvin's results[11], probably due to a difference in modeling of the cable junction at the "origin" or center of the hexagon, which shows appreciable motion in this mode.

References

1. Goldert, C. T., Lackey, J. A. and Spear, E. E., "Configuration Development of the Land Mobile Satellite System (LM SS) Spacecraft", NASA CP 2215, Part 2, 1981.

2. Pestle, E. C. and Leckie, F. A., "Matrix Methods in Elastomechanics", McGraw-Hill Book Co., Inc. 1963.

3. Leveseque, G., "Vibration Analysis of a Two Dimensional Model of Hoop/Column Antenna Satellite Configurations", M.S. Thesis, R. P. I., December 1984.

4. Sullivan, M. R., "(Hoop/Column Antenna Development Program", NASA CP-2269 Part 1, 1982.

5. Leader, B. J., "A Transfer Matrix Vibration Analysis of Some Components Typical of a Large Space Antenna", M.S. Thesis, R. P. I., December 1984.

6. Belvin H. K., NASA Langley Research Center, Private Correspondence to R. G. Loewy, R.P.I., Dated 3/25/85.

7. Elms, R.V., and Young, L.E., "SEP Solar Array Technology", 11th Intersociety Energy Conversion Engineering Conference, 1976.

8. Chidester, L.G., "Advanced Lightweight Solar Array Technology", AIAA Paper 78-533, Sep. 1978.

9. Chidester, L.G., "Advanced High Power Solar Array Technology", AIAA Paper 79-0884, May 1979.

10. Zaretzky, C. L., "Three-Dimensional Free Vibration Analysis of a Subassembly of the Hoop/Column Antenna Using the Transfer Matrix Method", M.S. Thesis, R. P. I., May 1987.

11. Belvin, W. K., "Vibration Characteristics of Hexagonal Radial Rib and Hoop Platforms:, Journal of Spacecraft and Rockets, Vol. 22, No. 4, July 1985, pp. 450-456.

12. Thomas, D. L., "Dynamics of Rotationally Periodic Structures", International Journal for Numerical Methods in Engineering, Vol. 14, 1979, pp. 81-102.

13. Zaretzky, C. L. and Loewy, R. G., "Transfer Matrix Analysis of Cable-Stiffened Hoop Platforms", accepted for publication (as of May 26, 1987) in the AIAA Journal of Spacecraft and Rockets.

14. Uhrig, R., "The Transfer Matrix Method Seen As One Method of Structural Analysis Among Others", Journal of Sound and Vibration, Vol. 4, 1966, pp. 136-148.

15. Davies, M. and Dawson, B., "A Distributed Element Method for Vibration Analysis of Flexible Spacecraft Based on Transfer Matrices", European Space Agency Journal, Vol. 9 , 1985, pp. 75-95.

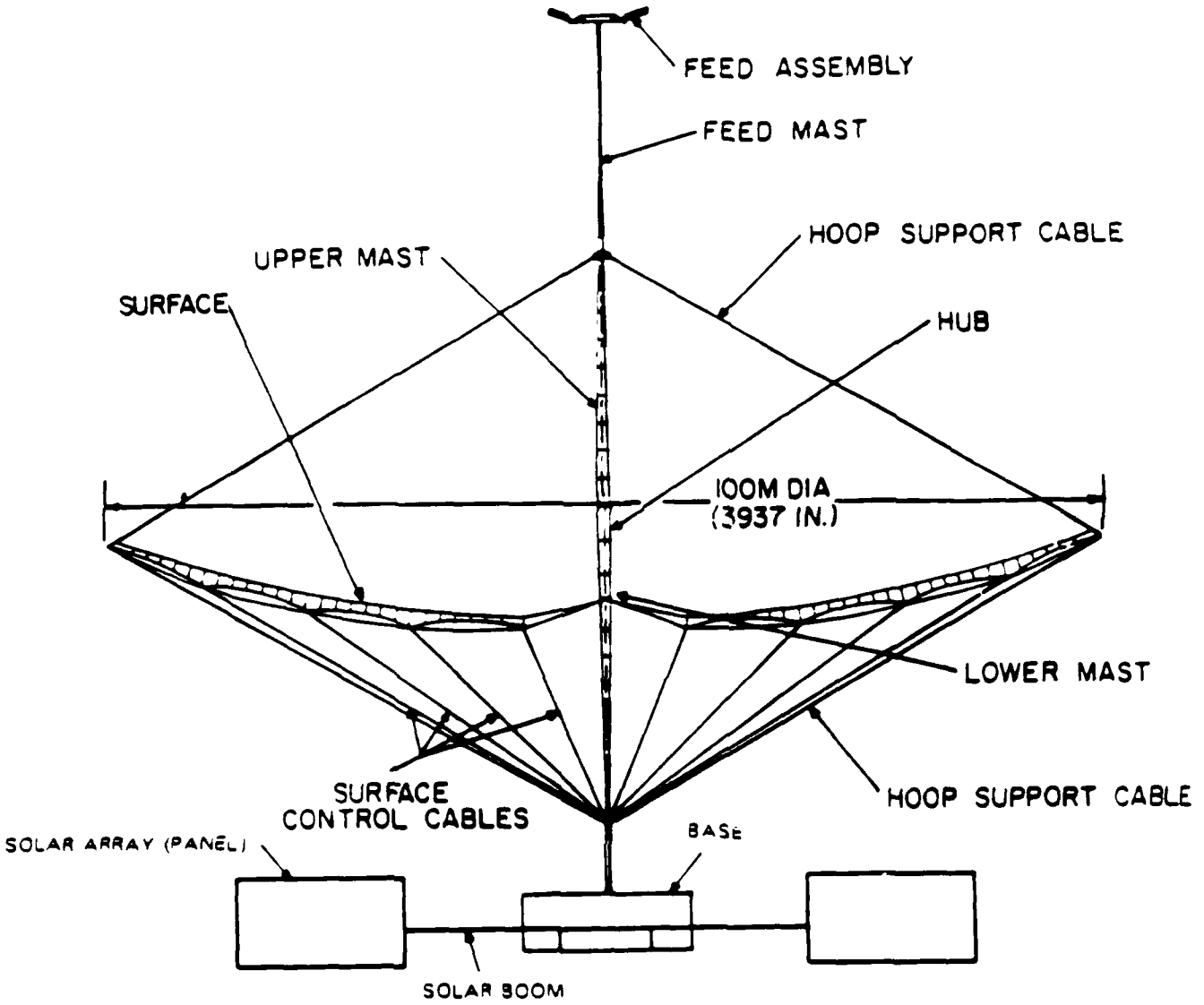

FIG. 1 Cross Section of Hoop-Column Antenna (Through Planes of Feed Assembly and Solar Panels.) (from Ref. #4)

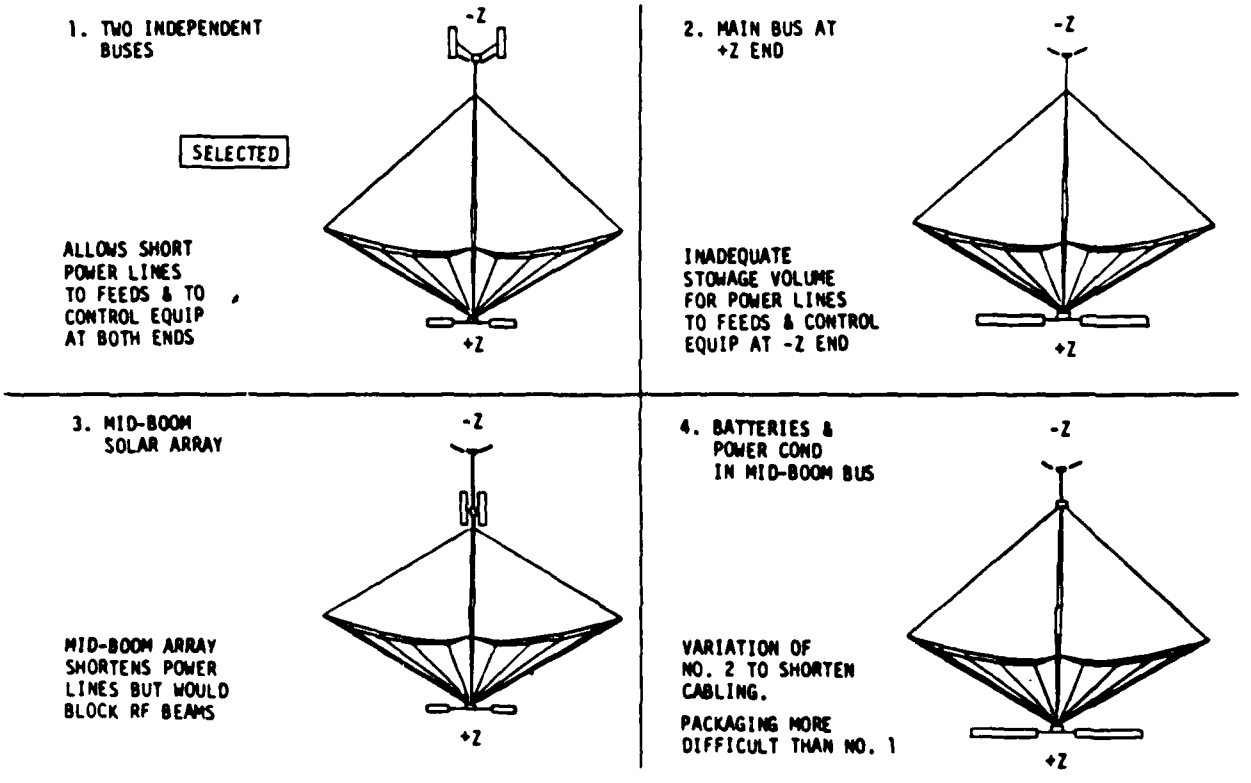

Fig. 2 Alternative Hoop Maypole Antenna Configurations (from Ref. 1)

Figure # 3a

- Bending Mode 1
- Axial Mode 1
- Bending Mode 2
- Bending Mode 3
- Bending Mode 4

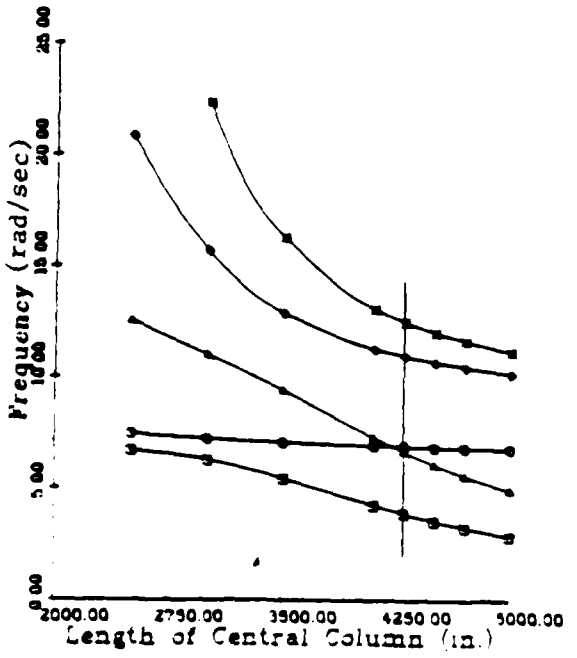

Figure # 4a

- Bending Mode 1
- Axial Mode 1
- Bending Mode 2
- Bending Mode 3
- Bending Mode 4

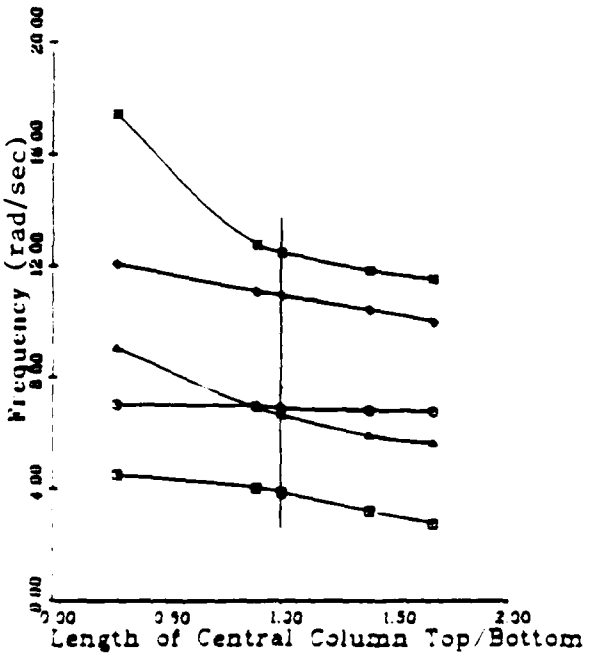

Figure # 3b

- Bending Mode 5
- Bending Mode 6
- Bending Mode 7
- Bending Mode 8

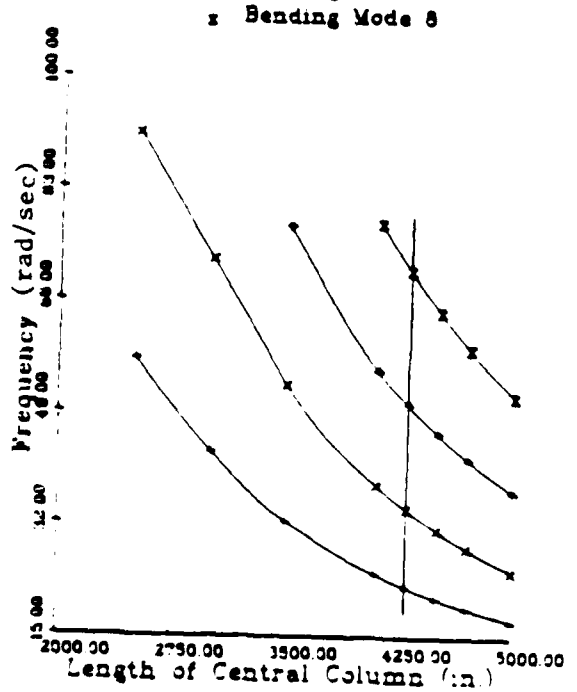

Figure # 4b

- Bending Mode 5
- Bending Mode 6
- Bending Mode 7
- Bending Mode 8

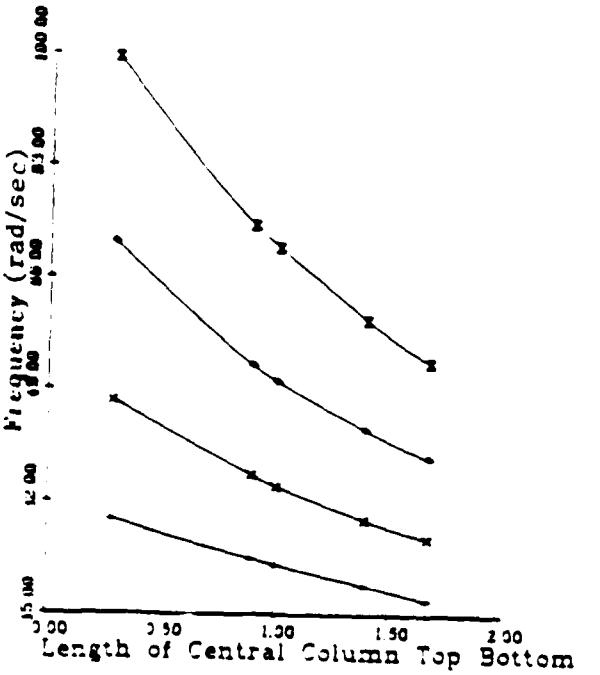

NB Bottom Mast Length is Constant

Figure # 5a

- Bending Mode 1
- Bending Mode 1 $P_A = \frac{1}{4} P_B$
- Bending Mode 2
- Bending Mode 2 $P_A = \frac{1}{4} P_B$
- Axial Mode 1

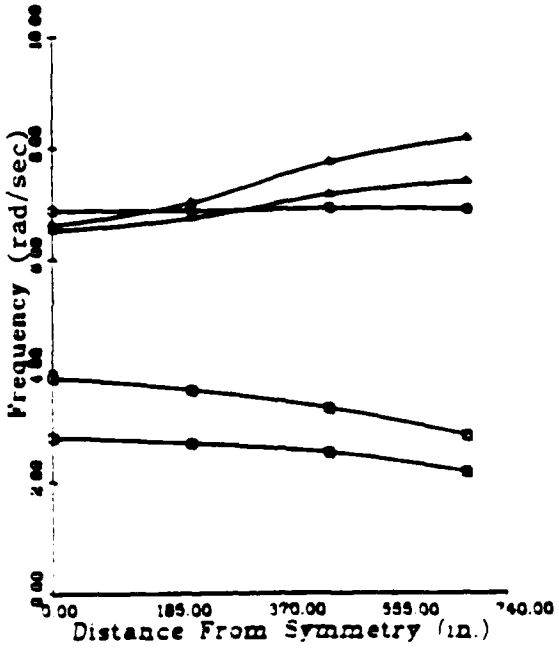

Figure # 5b

- Bending Mode 3
- Bending Mode 3 $P_A = \frac{1}{4} P_B$
- Bending Mode 4
- Bending Mode 4 $P_A = \frac{1}{4} P_B$
- Bending Mode
- Bending Mode 5 $P_A = \frac{1}{4} P_B$

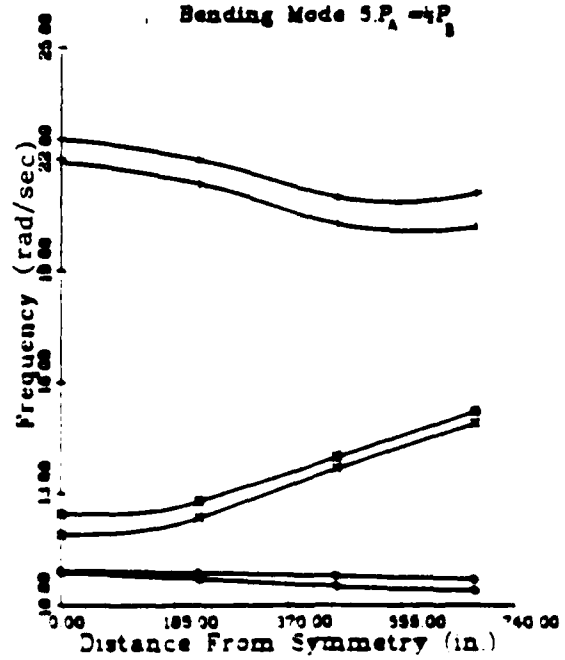

Figure # 6a
Bending Mode 1
Frequency= 3.8759 (rad/sec)
Mast Length= 4300.0
Displacement Scale= 500.00
Rigid Bar Length = 1000

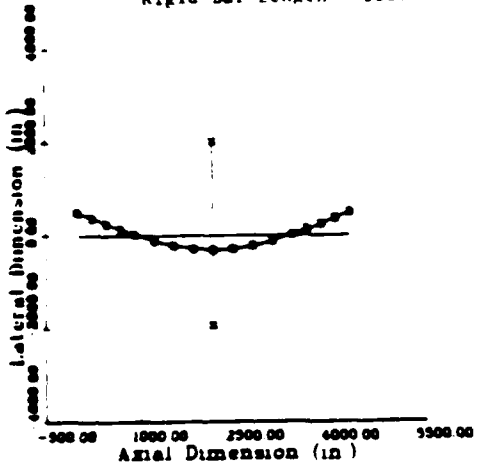

Figure # 6b
Bending Mode 3
Frequency= 9.1370 (rad/sec)
Mast Length= 4300.0
Displacement Scale= 500.00
Rigid Bar Length = 1000

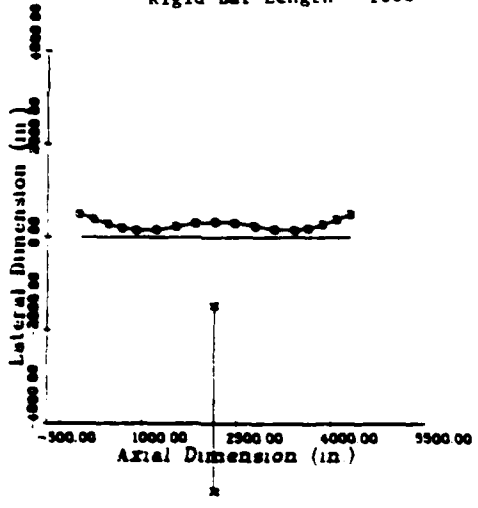

Figure # 6c
Bending Mode 5
Frequency= 21.0507 (rad/sec)
Mast Length= 4300.0
Displacement Scale= 500.00
Rigid Bar Length = 1000

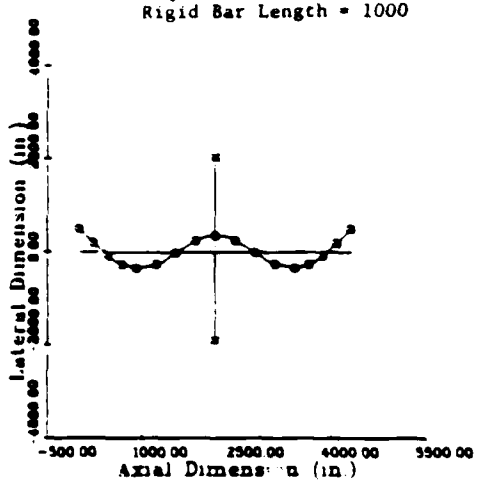

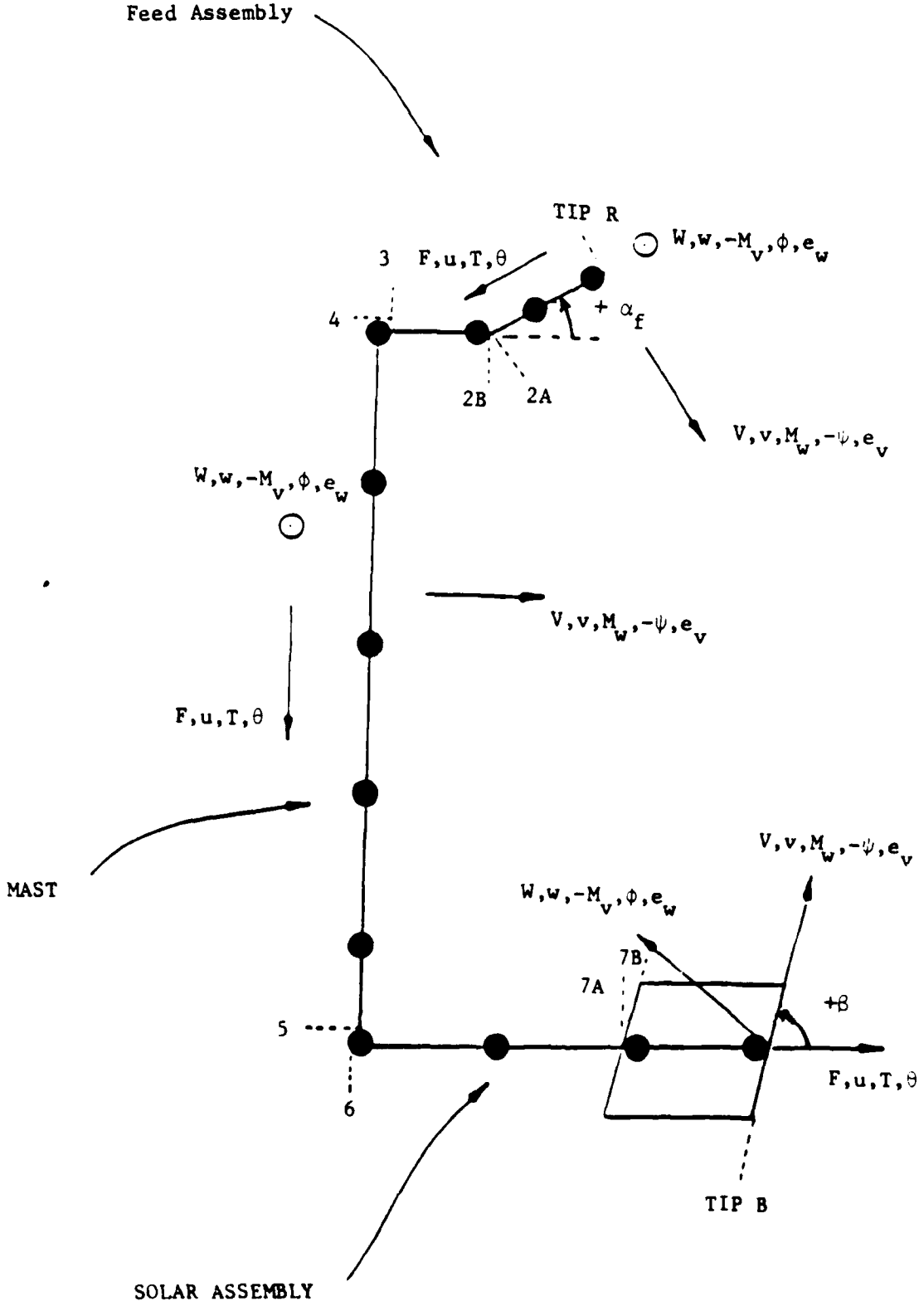

Fig. 7 Half-"H" Model (not to scale)

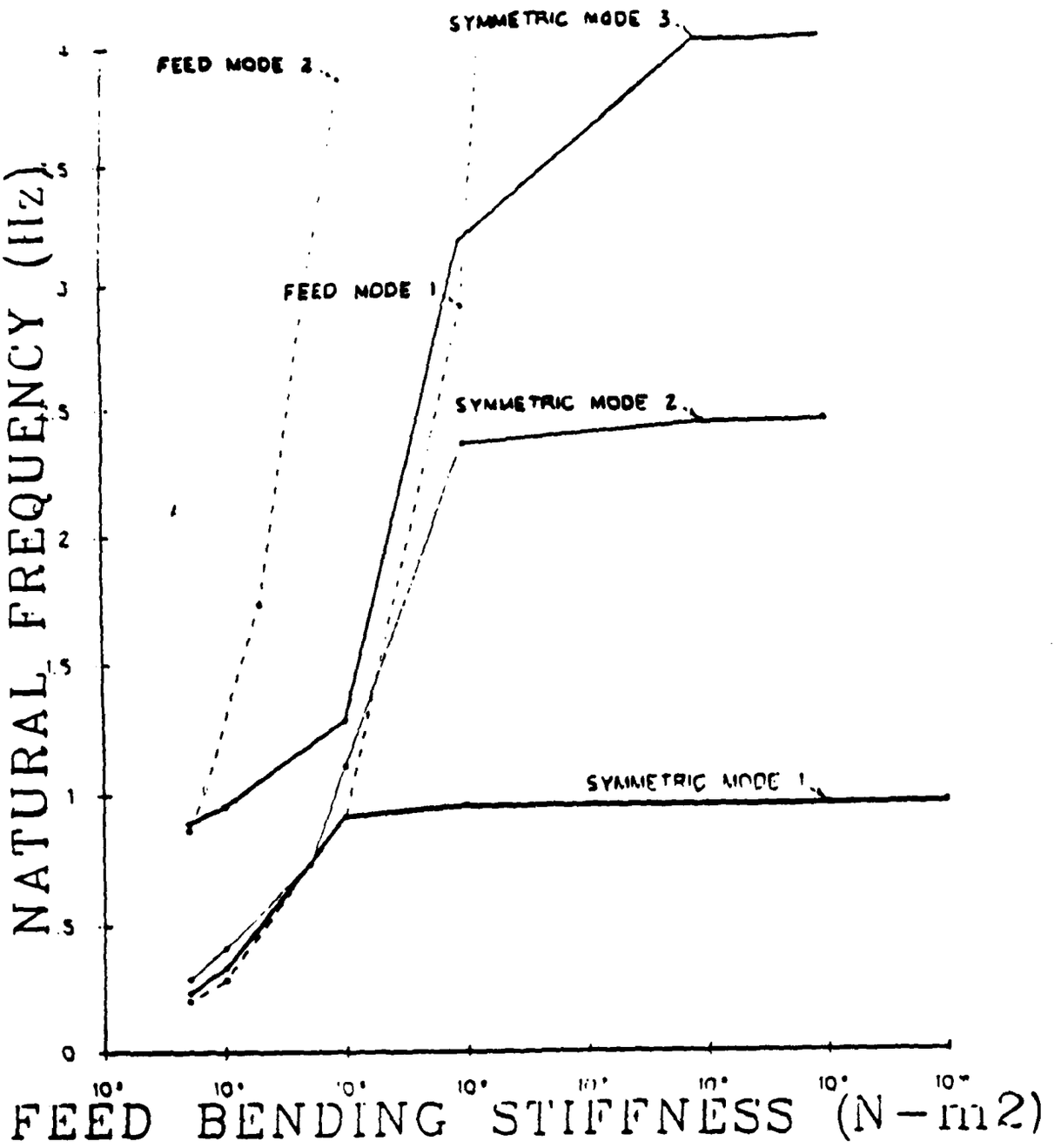

Fig. 8 Half-"H" Natural Frequency vx Feed Bending Stiffness-Symmetric Modes

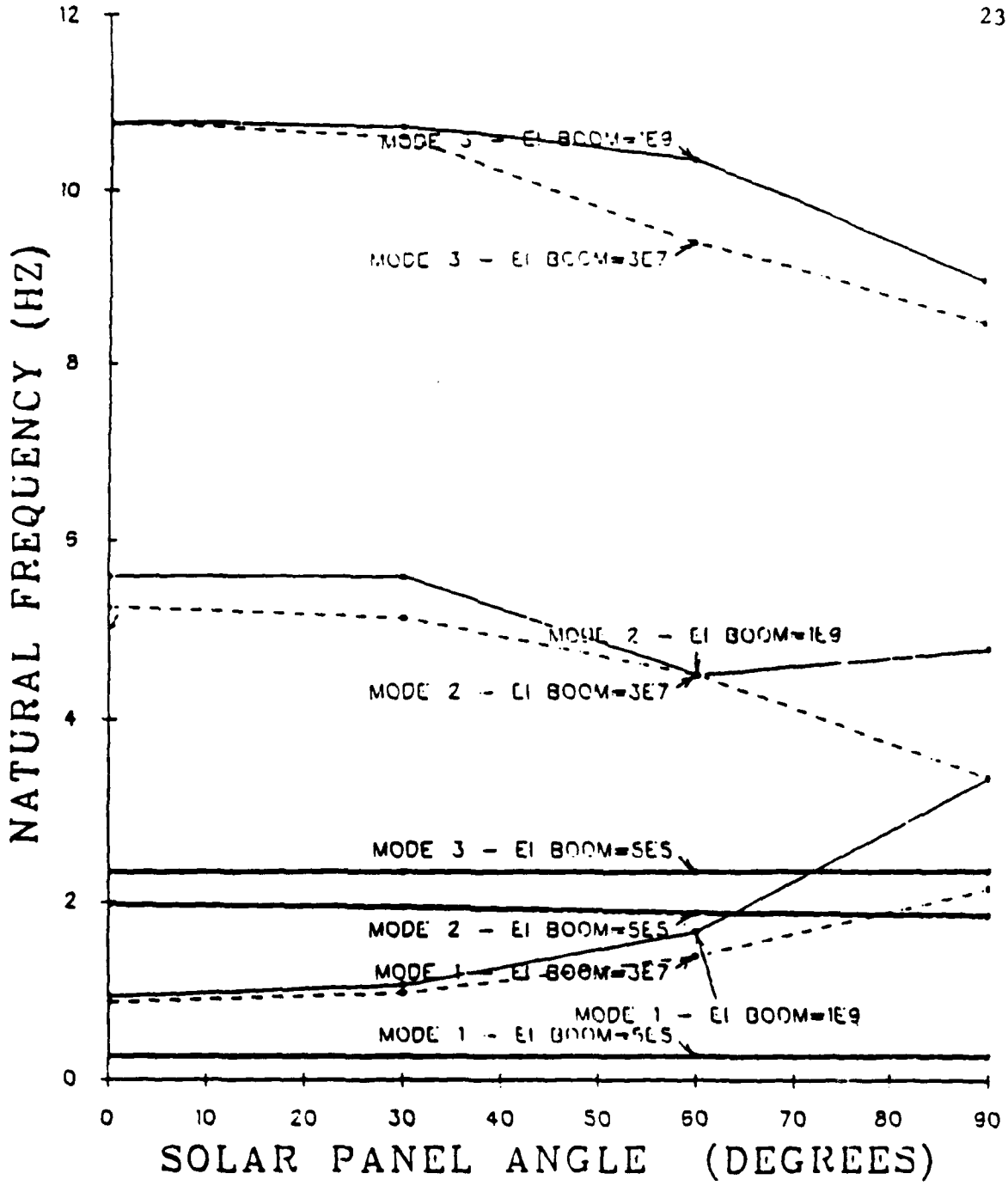

Fig. 9 Half-"H" Natural Frequency Vs. Solar Panel Cant For Various Values of Solar Boom Bending Stiffness - Antisymmetric Modes

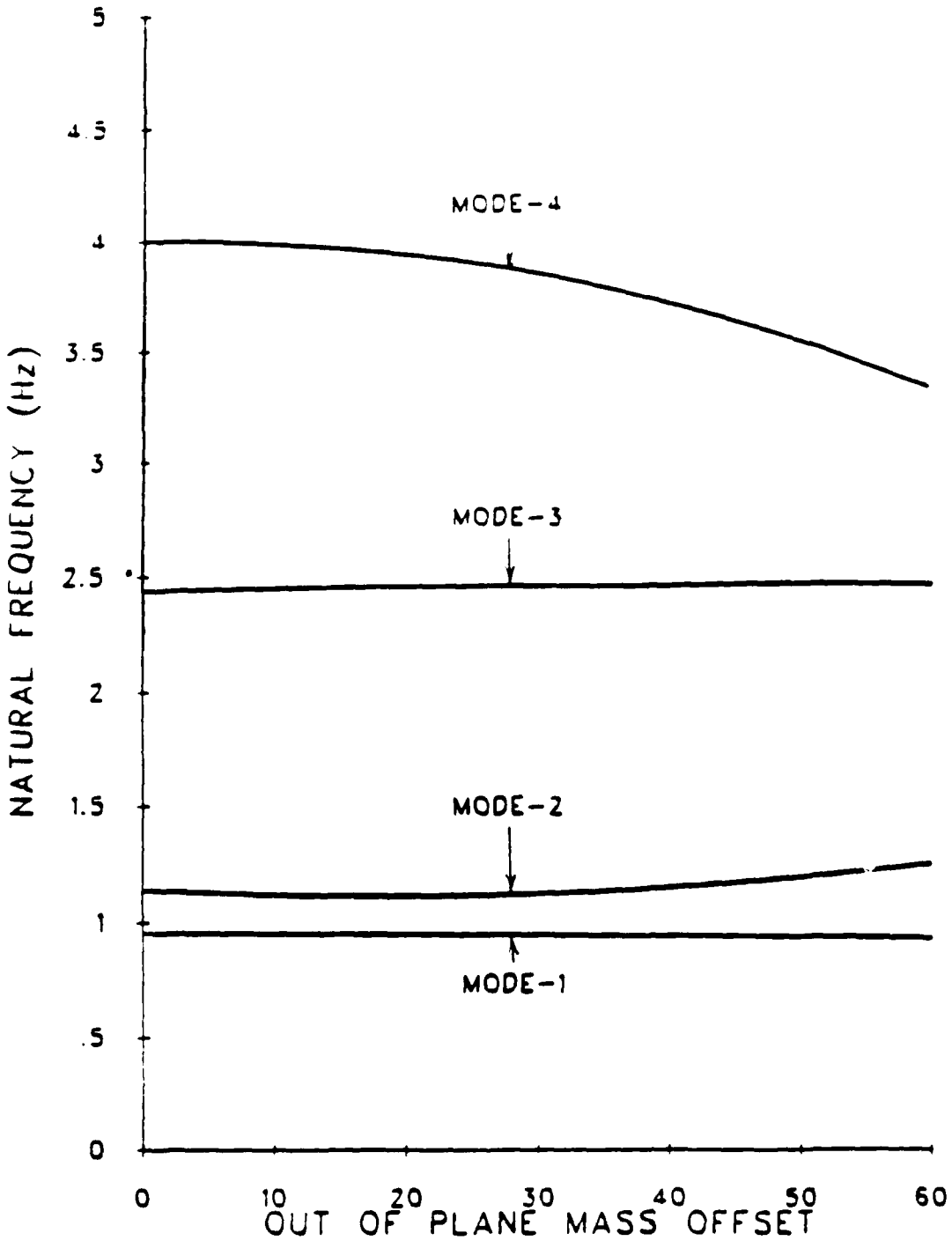

Fig. 10 Full-"H" Natural Frequency vs Out-Of-Plane Mass Offset Distance At "Top" of Mast

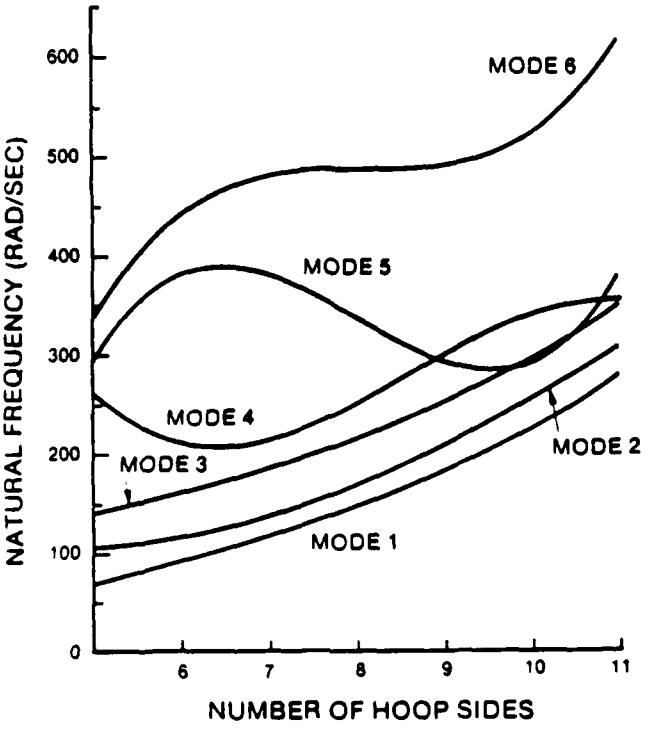

Fig. 11a In-plane Mode Frequencies for Polygonal Hoops (RAD = 1 m.)

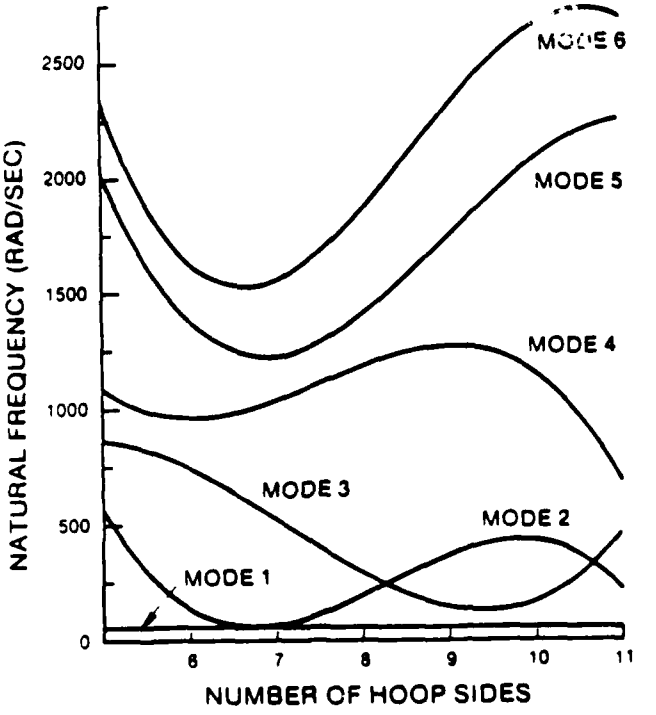

Fig. 11b Out-of-plane Mode Frequencies for Polygonal Hoops (RAD = 1 m.)

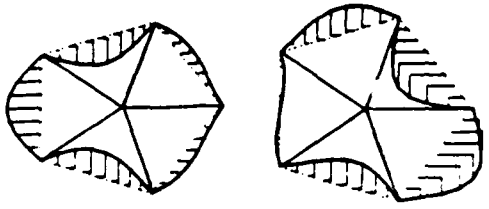

ω = 68.5 rad/sec

a. In-Plane
(Plan View)

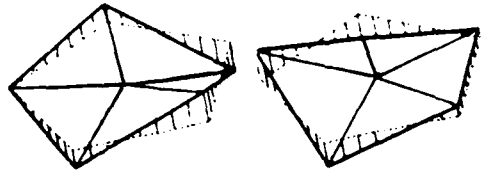

ω = 51. rad/sec

b. Out-of-Plane
(Isometric View)

Fig. 12 First Natural Mode Shapes for the Pentagonal, Cable-Stiffened Hoop

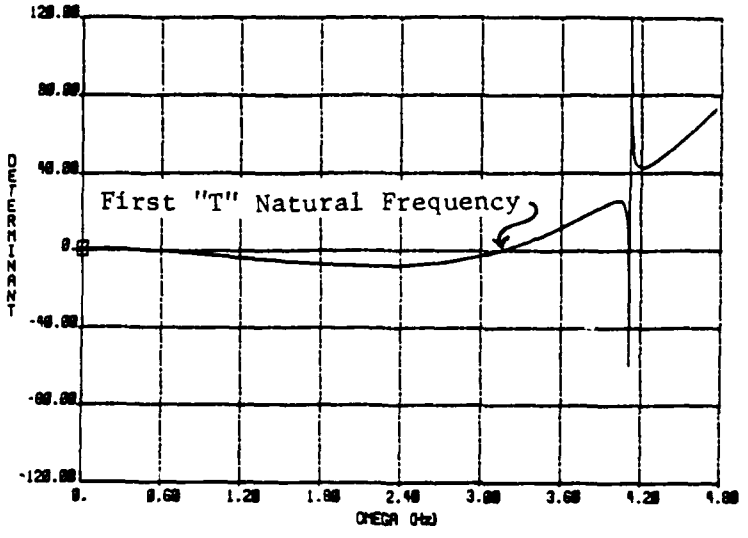

Fig. 13a Determinantal Value vs Trial Frequency Plot for a Full "T" Substructure

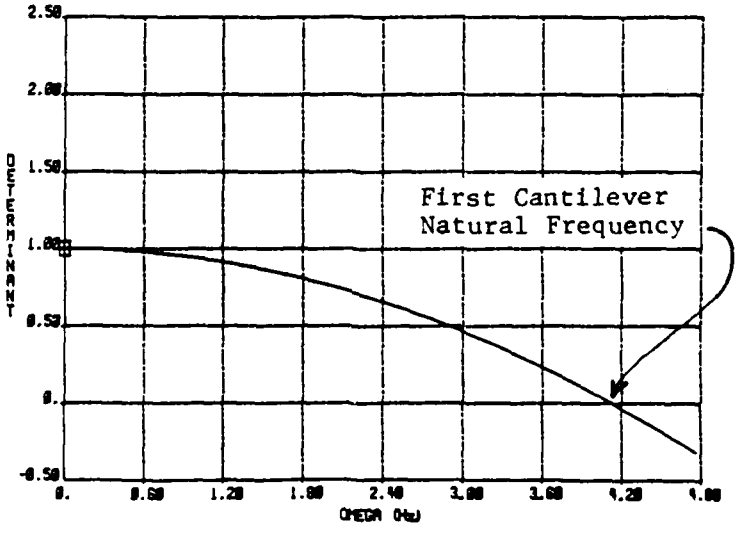

Fig. 13b Determinantal Value vs Trial Frequency Plot for One Side ot the "T's" Top, Cantilevered at the Juncture

END

12-87

DTIC